

An Approach of the Inverter Voltage Used for the Linear Machine with Multi Air-Gap Structure

Pierre Kenfack

Abstract—In this paper we present a contribution for the modelling and control of the inverter voltage of a permanent magnet linear generator with multi air-gap structure. The time domain control method is based on instant comparison of reference signals, in the form of current or voltage, with actual or measured signals. The reference current or voltage must be kept close to the actual signal with a reasonable tolerance. In this work, the time domain control method is used to control tracking signals. The performance evaluation concerns the continuation of reference signal. Simulations validate very well the tracking of reference variables (current, voltage) by measured or actual signals. All is simulated and presented under PSIM Software to show the performance and robustness of the proposed controller.

Keywords—Control, permanent magnet, linear machine, multi air-gap structure.

I. INTRODUCTION

THE production of energy is a major challenge for the years to come. Indeed, energy needs of industrialized societies are constantly increasing. Furthermore, developing countries will need more and more energy to carry out their development successfully. The consumption of these sources gives rise to greenhouse gas emissions and therefore an increase in pollution, rapid depletion and instability of fossil energy prices worldwide, and requires urgent research for new energy sources to meet current requirements. To meet the energy needs of today's society, it is necessary to find appropriate solutions and diversify them. Micro-cogeneration is one of the solutions. It is the simultaneous and decentralized production of heat and electricity at low power. The thermal and electrical powers produced make it possible to meet heating and electricity needs of buildings, ranging from single-family homes to tertiary and collective residential buildings. Used with renewable energies, micro-cogeneration thus enables to reduce not only the building's fossil energy consumption but also its greenhouse gas emissions. Micro-cogeneration will be done by our permanent magnet linear generator with a multi-air gap structure. Linear electrical machines with multi-air gap structure have an innovative place among unconventional electromechanical topologies [1], [2]. The aim is to increase the performance (force/displacement) of large linear electrical machines for direct drives. The idea is to fill the volume available for the linear electric machine as well as possible, in order to increase its volume performances. The linear electric machine consists of several more or less

independent elementary cells, each with its own active air gap zone. There is an increase in a given volume of the air gap surface. As the electromagnetic pressure is substantially maintained, the overall effort performance is increased.

Several approaches exist with regard to the study of the structure of the converter. We can mention the functional approach in which emphasis is placed on the study of electric models. We also have the functional structural approach which is based on the study of different power electronic sub-structures of which the converter is constituted [3]. The converter consists of a three-phase voltage inverter which is in fact only a VSC (Voltage Source Converter) connected to the DC voltage reserve [4]. In this paper, we wish to take advantage of the latest advances in control command and thus obtain high level performances by using converters intended to improve the transient stability of a micro-cogeneration connected to an infinite network. In order to analyze the influence of micro-cogeneration on the grid, a mathematical model of the converter connected to an electrical grid will be studied.

II. MULTI AIR-GAP STRUCTURE

All previous solutions are inappropriate when important strokes are required, typically for a few tens of millimeters and more, especially if the aim is to be competitive with a fluid-pressure device in the mass or volume. The first can provide the force but not the stroke, the second can provide the stroke but with less force. An original solution to have a specific effort of more than one hundred of N/kg is to act on the active surface: the air gap surface. The original solution allows not reducing the stroke, and using the normal or tangential magnetic pressure, inherently limited to weak values. The objective is then to maximize the surface by multiplying the numbers of fixed and mobile parts within a given volume.

This structure is achieved from asynchronous or synchronous machines with variable reluctance or permanent magnets. Multi air-gap structure uses the tangential component of the magnetic pressure, but solutions with permanent magnets give the best result. Fig. 1 illustrates this initiative using a permanent magnet synchronous structure derived from a conventional cylindrical machine with rotating magnetic field. In this structure with 4 air gaps, mobile parts, also known sliders later, are formed of two plates madding up alternating permanent magnets. Stators are made up of slotted sheet assembly, and filled by single or multi-phase windings for creating travelling field.

Kenfack Pierre is with the University of Buea, Higher Teachers Technical Training College (HTTC) Kumba, Cameroon (phone: +23793448422; e-mail: pierrekenfack2003@yahoo.fr).

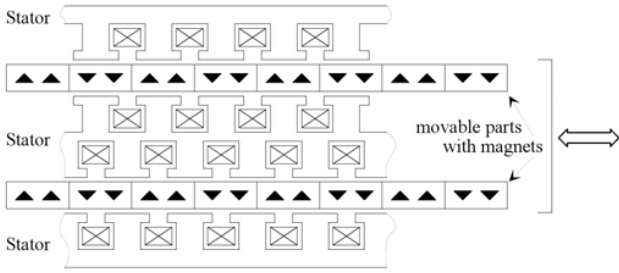


Fig. 1 Multi air-gap structure

III. INVERTER MODELLING

The inverter is nothing other than a VSC which is a three-phase voltage converter consisting of 3 switch arms and connected to the grid via a three-phase transformer [3]. Each switch arm consists of a combination of two blocks each having a controllable switch (Insulated-Gate Bipolar Transistor) for example mounted in parallel placed freewheeling diode and having the role of blocking reverse voltages. Its role is to rectify the AC power from the transformer and send it to the DC circuit [5]. In addition to this, it also performs the reactive power compensation function since it can supply or absorb reactive power, independently of the active power, to the network [6]-[10]. The inverter is modeled by ideal switches. The only constraint is the floating neutral. The voltages U_a, U_b and U_c correspond to the string voltages of the three-phase inverter. The voltages U_{a1}, U_{b1} and U_{c1} are phase voltages of the inverter Fig 2.

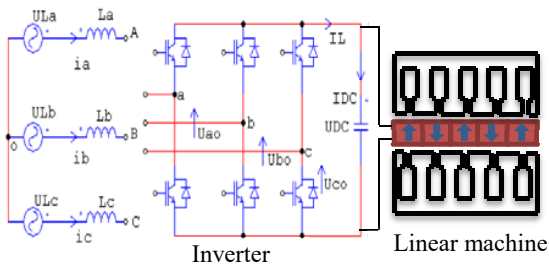


Fig. 2 Linear machine with inverter

The voltages U_a, U_b and U_c can be imposed by an appropriate control of the electronic switches (static contactors) [11], [12]. The voltages U_{k0} (with $k=a, b$ and c) can be determined at the inverter output. We have:

$$\begin{cases} U_{a1} - U_{a0} - U_{b1} + U_{b0} = 0 \\ U_{a1} - U_{a0} - U_{c1} + U_{c0} = 0 \end{cases} \quad (1)$$

Depending on the conduction of the switches in an inverter string, the string voltages U_{k0} can be equal to either U_{DC} or 0. The network being symmetrical three-phase with floating neutral point, we have:

$$\begin{cases} U_a + U_b + U_c = 0 \\ i_a + i_b + i_c = 0 \end{cases} \quad (2)$$

$$\begin{bmatrix} U_{a1} \\ U_{b1} \\ U_{c1} \end{bmatrix} = \frac{1}{3} \begin{bmatrix} 2 & -1 & -1 \\ -1 & 2 & -1 \\ -1 & -1 & 2 \end{bmatrix} \begin{bmatrix} U_{a0} \\ U_{b0} \\ U_{c0} \end{bmatrix} \quad (3)$$

For the three phase voltages of the circuit, we have (4) and (5) using the definition of the space vector. The general relationship is given by (6).

$$\begin{bmatrix} U_a \\ U_b \\ U_c \end{bmatrix} = \begin{bmatrix} L_a & 0 & 0 \\ 0 & L_b & 0 \\ 0 & 0 & L_c \end{bmatrix} \begin{bmatrix} \frac{di_a}{dt} \\ \frac{di_b}{dt} \\ \frac{di_c}{dt} \end{bmatrix} + \begin{bmatrix} U_{a1} \\ U_{b1} \\ U_{c1} \end{bmatrix} \quad (4)$$

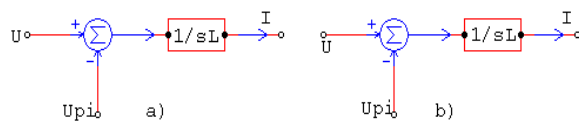
$$\begin{cases} U(t) = U_{a1}(t) + aU_{b1}(t) + a^2U_{c1}(t) \\ I(t) = i_a(t) + ai_b(t) + a^2i_c(t) \end{cases} \quad a = e^{j2\pi/3} \quad (5)$$

$$U(t) = L \frac{di(t)}{dt} + U_i(t) \quad L_a = L_b = L_c = L \quad (6)$$

Taking into account (6) transformation from natural abc to stationary $\alpha\beta$ coordinate system can be expressed as:

$$\begin{cases} U_\alpha(t) = L \frac{di_\alpha}{dt} + U_{i\alpha}(t) \\ U_\beta(t) = L \frac{di_\beta}{dt} + U_{i\beta}(t) \end{cases} \quad (7)$$

Fig. 3 illustrates the structural diagram of such a representation.



$$\begin{aligned} a) \quad i_\alpha(t) &= \frac{1}{sL} (U_\alpha - U_{pi\alpha}) \\ b) \quad i_\beta(t) &= \frac{1}{sL} (U_\beta - U_{pi\beta}) \end{aligned}$$

Fig. 3 Structural diagram

The voltage of the inverter (U_a, U_b, U_c) depends on the state of the switches (S_a, S_b, S_c) and the DC voltage U_{DC} , (8) and the current I_L is the sum of the currents of each line given by (9).

$$U_p = U_{DC} (S_k - \frac{1}{3} \sum S_k) \quad k = a, b, c \quad (8)$$

$$I_L = i_a S_a + i_b S_b + i_c S_c \quad (9)$$

The current flowing through the capacitor is obtained by the (10). I_g : Linear generator current.

$$\begin{cases} I_{DC} = I_L - I_g \\ C \frac{dU_{DC}}{dt} + \frac{U_{DC}}{R} = i_a S_a + i_b S_b + i_c S_c \end{cases} \quad (10)$$

After decomposition of space vectors into α and β components, one obtains:

$$\begin{cases} \begin{bmatrix} U_\alpha \\ U_\beta \end{bmatrix} = \frac{2}{3} \begin{bmatrix} 1 & \cos\left(\frac{2\pi}{3}\right) & \cos\left(\frac{4\pi}{3}\right) \\ 0 & \sin\left(\frac{2\pi}{3}\right) & \sin\left(\frac{4\pi}{3}\right) \end{bmatrix} \begin{bmatrix} U_{L_a} \\ U_{L_b} \\ U_{L_c} \end{bmatrix} \\ \frac{C}{2} \frac{dU_{DC}^2}{dt} + \frac{U_{DC}^2}{R} = \frac{3}{2} U_m I_m \end{cases} \quad (11)$$

Equation (11) in stationary coordinates α and β , allows us to obtain the global ordering strategy, Fig 4.

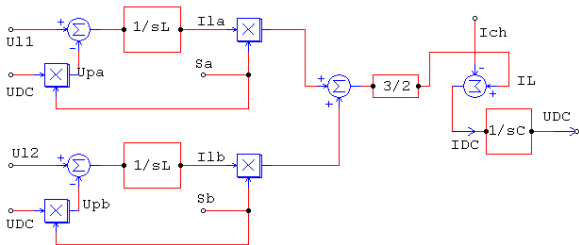


Fig. 4 Overall structural diagrams

To reduce the effects of the harmonics, carrier based PWM techniques are used. It consists in changing the pulse width of the output voltage with appropriate controls of the switches, comparing the sinusoidal reference signal with a triangular carrier wave of frequency f_c [13]-[15], Fig5.

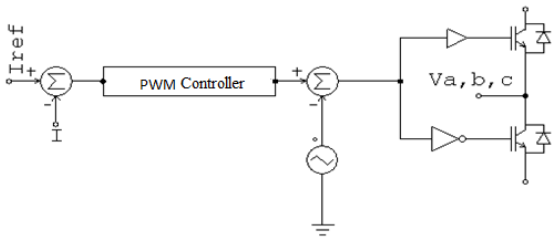


Fig. 5 PWM current control

The PWM allows the inverter to generate an output wave very close to the ideal shape and to obtain linear control of the amplitude of the output voltage and current. Fig. 5 illustrates the PWM controller calculation structure. We will use a P.I, taking a bandwidth less than or equal to half a decade of the cut-off frequency ($\omega_p = \omega_c / (10)^{1/2}$), we deduce

$$K = L * \omega_p \text{ and } T_i = (10)^{1/2} / \omega_p. \text{ Carrier frequency: } 10 \text{ kHz.}$$

Fig. 6 shows the calculation block for the voltage controller. The controller action will be to maintain the average value of the output voltage and not the instantaneous value. The calculation of voltage controller is done using (12) and the transfer function, (13):

$$\frac{3}{2} U_m I_m = U_{DC0} \left(C \frac{dU_{DC0}}{dt} + \frac{U_{DC0}}{R} \right) \quad (12)$$

$$\frac{\delta U_{DC0}}{\delta I_m} = \frac{3}{2} U_m \frac{R}{1 + \frac{RC}{2}s} \quad (13)$$

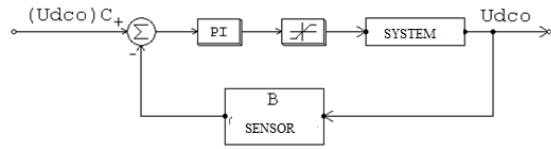


Fig. 6 Voltage controller calculation block

Let us calculate the gain K and the integration time

$$T_i (C(p) = K(1+T_i.p)/T_i.p). K * T_i = R * C / 2$$

$$1/2\pi f_p = T_i / (3/2) * U_m . R . B,$$

B is the sensor. The voltage cut-off frequency is adjusted to 20 Hz. The PI controller: $K = 1.855$; $T_i = 2.695 \text{ msec}$.

IV. RESULTS

Several simulations have been done in order to evaluate described control methods. Simulations have been focused on time domain.

TABLE I
MAIN DATA OF SIMULATION MODEL

Symbol	Quantity	Units	Value
f	frequency	Hz	50
V_{L-L}	supply voltage	V	400
L	inductance	mH	5
C	DC-link capacitance	μF	200

The control method in the time domain is based on the instant comparison of the reference signals in Fig. 7, in the form of current or voltage, with the actual or measured signals in Fig. 8.

The reference current is kept close to the measured signal shown in Fig. 9, as is the DC bus voltage in Fig. 10. The simulation results validate very well the tracking of the reference variables (current, voltage) by the measured or actual signals.

V. CONCLUSION

In the literature, several mathematical models [3]-[11] of the inverter are proposed for functional analysis and different simulations. The selected inverter model will be governed by (11)-(13). The generation of reference signals used to control the opening and closing of the inverter semiconductors is carried out using control algorithms that can be classified into time, frequency or other domains (fuzzy logic, predictive control, etc.).

The time domain control method is used to control the tracking signals. The evaluation concerns the continuation of the reference signal. The simulations presented under PSIM software validate very well the tracking of the reference variables (current, voltage) by the measured or actual signals.

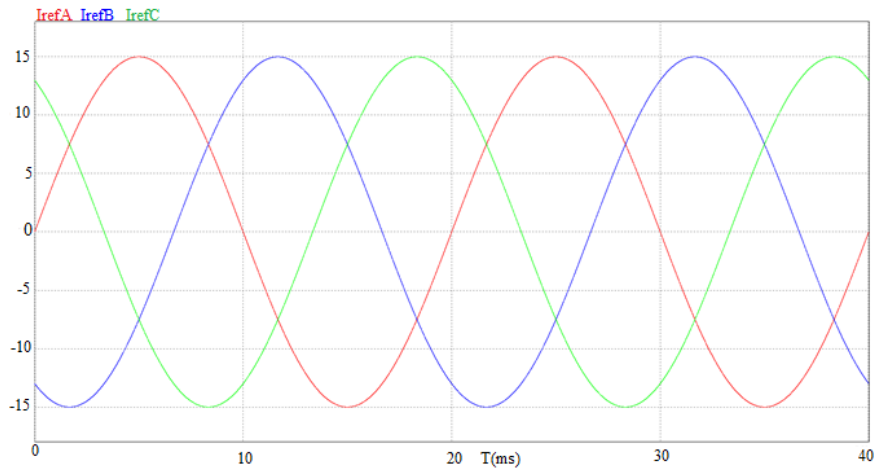


Fig. 7 Reference currents (I_{refA} , I_{refB} , I_{refC})

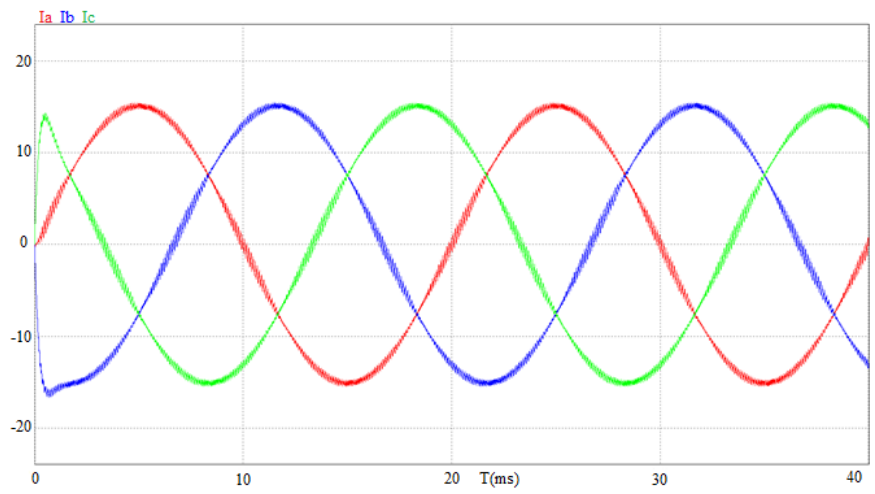


Fig. 8 Measured currents (I_a , I_b , I_c)

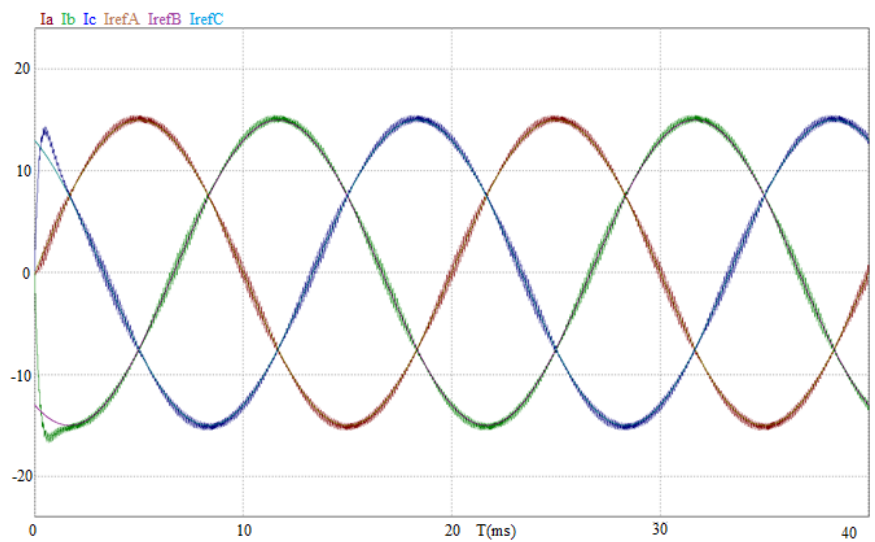


Fig 9 Current tracking (I_k measured currents, I_{refK} with $k= a,b, c$ reference currents)

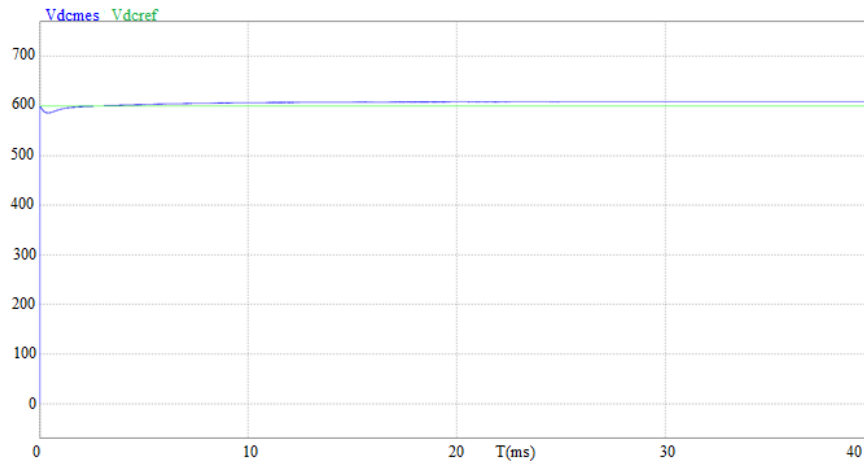


Fig 10 Voltage tracking (V_{dcmes} : measured voltage, V_{dcref} : reference voltage)

REFERENCES

- [1] Pierre Kenfack, Daniel Matt, Philippe Enrici, Designing a Permanent Magnet Linear Generator Multi Air-gap Structure using the Finite Element Method, 10th International Conference on Electrical and Electronics Engineering (ELECO 2017), 30 November - 2 December 2017, Bursa-Turkey (2017) PP: 1414-1418. Electronic ISBN: 978-605-01-1134-7 IEEE.
- [2] P. Kenfack, D.Matt, P.Enrici, M.François, Impact of Mechanical Stresses on Flat double sided Linear Electric Motor Multi-air gap Structure guided or Friction Plates, IEEE International Magnetics Conference (INTERMAG Europe 2017), 24th – 28th April 2017, Dublin-Ireland (2017). Electronic ISSN: 2150-4601 IEEE.
- [3] E.Gholipour Sharaki, Apport de l'UPFC à l'amélioration de la stabilité transitoire des réseaux électriques, Thèse de Doctorat de l'Université Henri Poincaré, Nancy I, 13 octobre 2003.
- [4] E. Catz, Evolutions techniques du système de transport et de distribution d'électricité, in *J3eA*, Vol. 5 Hors-Série, 2006.
- [5] T. Wildi, *Electrotechnique*, Les presses de l'université Laval, Québec et Ottawa, 2001. Ch.42
- [6] N.F. Mailah, S.M. Bashi, Single phase Unified Power Controller (UPFC): Simulation and construction, European Journal of Scientific Research, vol.30 No.4, PP.677-684, 2009.
- [7] G.S. Perantzakis, and al, A predictive Current Control Technique for Three- Level NPC Voltage Source Inverters, 0-7803-9033-4/05/2005 IEEE.
- [8] Le Jiang-yuan, Zhang Zhi, Lai Xiao-hua Jiang, Predictive direct power control of three-phase shunt active power filter, Electric Machines and Control, 2012.16(5): 86-90.
- [9] Li Ning, Wang Yue, WANG Zhao-an, Reviews of Direct Power Control Strategy in Power Electronic Converters, Journal of Supply. 2013.1(1):45-52.
- [10] Guangqing Bao, Jingyi Wen, Xiaolan Wang, Dongsong Luo, Predictive Direct Power Control for Permanent Magnet Linear Generator Side Converter, 17th International Conference on Electrical Machines and Systems (ICEMS), Oct. 22-25, 2014, Hangzhou, China.
- [11] Vladimir Blasko *Member, IEEE*, Vikram Kaura *Member, IEEE*, A New Mathematical Model and Control of a Three- Phase AC- DC Voltage Source Converter, IEEE Transactions on Power Electronics, Vol. 12, No. 1, January 1997.
- [12] Yun Wei Li *Member, IEEE*, Control and Resonance Damping of Voltage –Source and Current- Source Converters With LC Filters, IEEE Transactions on Power Electronics, Vol. 56, No. 5, May 2009.
- [13] H. Buhler, *Convertisseurs statiques*, PPUR 1991, Lausanne, Switzerland.
- [14] Y.Ye, M. Kazerani, V.H. Quintana, A Novel Modeling and Control Method for Three-Phase PWM Converters, 0-7803-7067-8/01/2001 IEEE.
- [15] Y Yang Xing-wu, Jiang Jian-guo. Predictive direct power control for three-phase voltage source PWM rectifiers. Proceedings of the CSEE, 2011.31(3):34-39.